

**Supporting Information for**  
High-throughput Screen Identifies Non-Inflammatory Small Molecule  
Inducers of Trained Immunity

Hannah Riley Knight<sup>1</sup>, Ellen Ketter<sup>2</sup>, Trevor Ung<sup>1</sup>, Adam Weiss<sup>1</sup>, Jainu Ajit<sup>1</sup>, Qing Chen<sup>1</sup>, Jingjing Shen<sup>1</sup>, Ka Man Ip<sup>2</sup>, Chun-yi Chiang<sup>2</sup>, Luis Barreiro<sup>2</sup>, Aaron Esser-Kahn<sup>\*1</sup>

\*Aaron Esser-Kahn

Email: [aesserkahn@uchicago.edu](mailto:aesserkahn@uchicago.edu)

**This PDF file includes:**

Key Resources Table  
Figures S1 to S4  
Legends for Datasets S1-S4

**Other supporting materials for this manuscript include the following:**

Datasets S1-S4

| REAGENT or RESOURCE                                    | SOURCE                  | IDENTIFIER  |
|--|-------------------------|---|
| <b>Antibodies</b>                                      |                         |   |
| Purified anti-mouse CD16/32 Antibody                   | BioLegend               | AB_312801 (BioLegend Cat. No. 101302)   |
| Alexa Fluor® 647 anti-mouse TNF- $\alpha$ Antibody     | BioLegend               | AB_493330 (BioLegend Cat. No. 506314)   |
| PE anti-mouse IL-6 Antibody                            | BioLegend               | AB_315338 (BioLegend Cat. No. 504504)   |
| APC/Cyanine7 anti-mouse CD45 Antibody                  | BioLegend               | AB_312981 (BioLegend Cat. No. 103116)   |
| BD Horizon™ BUV737 Rat Anti-CD11b                      | BD Biosciences          | AB_2738811 (BD Cat. No. 612800)   |
| Brilliant Violet 650™ anti-mouse CD11c Antibody        | BioLegend               | AB_2562414 (BioLegend Cat. No. 117339)  |
| BD Horizon™ BUV395 Rat Anti-Mouse F4/80                | BD Biosciences          | AB_2739304 (BD Cat. No. 565614)   |
| Alexa Fluor® 700 anti-mouse Ly-6C Antibody             | BioLegend               | AB_10643270 (BioLegend Cat. No. 128024)   |
| Brilliant Violet 421™ anti-mouse Ly-6G Antibody        | BioLegend               | AB_2562567 (BioLegend Cat. No. 127628)  |
| APC/Fire™ 810 anti-mouse NK-1.1 Antibody               | BioLegend               | AB_2894654 (BioLegend Cat. No. 156519)  |
| PE/Cyanine7 anti-mouse CD170 (Siglec-F) Antibody       | BioLegend               | AB_2890715 (BioLegend Cat. No. 155528)  |
| PerCP/Cyanine5.5 anti-mouse I-A/I-E Antibody           | BioLegend               | AB_2191071 (BioLegend Cat. No. 107626)  |
| Brilliant Violet 605™ anti-mouse CD86 Antibody         | BioLegend               | AB_11204429 (BioLegend Cat. No. 105037)   |
| PE/Dazzle™ 594 anti-mouse CD40 Antibody                | BioLegend               | AB_2572185 (BioLegend Cat. No. 124630)  |
| Alexa Fluor® 488 anti-mouse CD3 Antibody               | BioLegend               | AB_389301 (BioLegend Cat. No. 100210)   |
| Brilliant Violet 785™ anti-mouse CD19 Antibody         | BioLegend               | AB_11218994 (BioLegend Cat. No. 115543)   |
| <b>Chemicals, peptides, and recombinant proteins</b>   |                         |   |
| Microsource Spectrum Collection Small Molecule Library | Discovery Systems, Inc. | <a href="http://www.msdiscovery.com/spectrum.html">http://www.msdiscovery.com/spectrum.html</a> |
| Flunisolid   | Sigma-Aldrich           | Cat. No. F5201  |
| 5-fluoroindole-2-carboxylic acid                       | Thermo Scientific       | Cat. No. AC331590010  |
| Myricetin  | Selleck Chemicals       | Cat. No. S2326  |
| Hydrocortisone   | Selleck Chemicals       | Cat. No. S1696  |
| Nerol  | Selleck Chemicals       | Cat. No. S4970  |
| Hydroquinone   | Selleck Chemicals       | Cat. No. S4580  |
| Fenoterol Hydrobromide                                 | Sigma-Aldrich           | Cat. No. f1016  |
| Recombinant Mouse IFN- $\gamma$ (carrier-free)         | BioLegend               | Cat. No. 575308   |
| Pam3CSK4 VacchiGrade                                   | Invivogen               | Cat. No. vac-pms  |
| LPS-B5 Ultrapure                                       | Invivogen               | Cat. No. tlrl-pb5lps  |
| 5'-deoxy-5'-(methylthio)adenosine                      | Sigma-Aldrich           | Cat. No. D5011  |
| (-)-epigallocatechin-3-gallate                         | Sigma-Aldrich           | Cat. No. E4143  |
| 2' deoxy-D-glucose                                     | Sigma-Aldrich           | Cat. No. D3179  |
| Corn Oil   | Sigma-Aldrich           | Cat. No. C8267  |
| 0.1% IGEPAL CA-630                                     | abcam                   | Cat. No. ab285400   |

|  |                          |   |
|--|--------------------------|---|
| GolgiPlug  | BD Biosciences           | Cat. No. 555029   |
| GolgiStop  | BD Biosciences           | Cat. No. 554724   |
| Live/Dead Aqua   | Thermo Fisher Scientific | Cat. No. L34966   |
| Critical commercial assays                             |                          |   |
| Mouse TNF- $\alpha$ ELISA MAX <sup>TM</sup> Deluxe Kit | BioLegend                | Cat. No. 430904   |
| Mouse IL-6 ELISA MAX <sup>TM</sup> Deluxe Kit          | BioLegend                | Cat. No. 431304   |
| MinElute PCR Purification Kit                          | Qiagen                   | Cat. No. 28004  |
| Tagment DNA Enzyme and Buffer                          | Illumina                 | Cat. No. 20034197   |
| TG Nextera <sup>®</sup> XT Index Kit v2 Set A          | Illumina                 | Cat. No. TG-131-2001  |
| Cytofix/Cytoperm                                       | BD Biosciences           | Cat. No. 555028   |
| Deposited data   |                          |   |
| Raw fastq files, ATACseq                               | GEO                      | Original sequencing data  |
| ATACseq analysis code                                  | GitHUB                   | @ellenketter  |
| Experimental models: Cell lines                        |                          |   |
| Hek-Blue TNF- $\alpha$ Cells                           | Invivogen                | Cat. No. hkb-tnfdmyd  |
| L929 Cells   | ATCC                     | Cat. No. ccl-1  |
| Experimental models: Organisms/strains                 |                          |   |
| C57BL/6 mice   | Jackson Laboratory       | IMSR_JAX:000664   |
| Software and algorithms                                |                          |   |
| GraphPad Prism   | Dotmatics                | <a href="https://www.graphpad.com/">https://www.graphpad.com/</a>   |
| FlowJo   | Becton Dickinson         | <a href="https://www.flowjo.com/">https://www.flowjo.com/</a>       |
| BioRender  | BioRender                | <a href="https://www.biorender.com/">https://www.biorender.com/</a> |

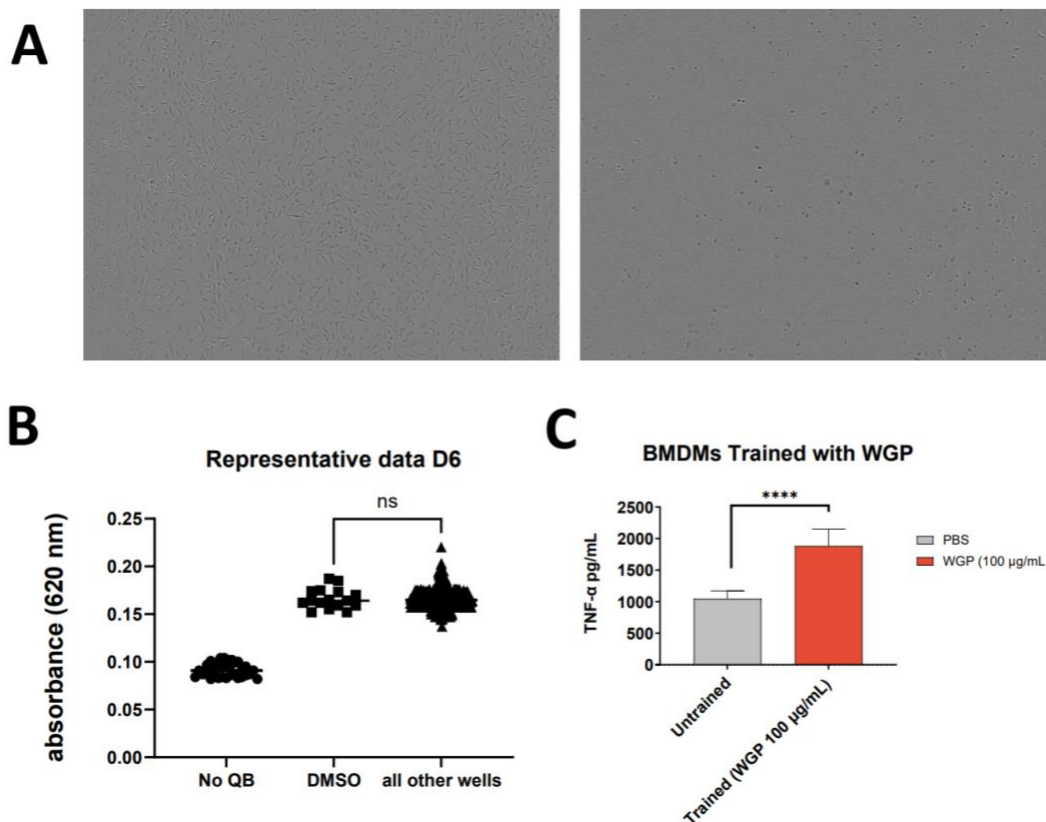


**Fig. S1.** A) IncuCyte quantifies viability based on cellular confluence. Example images in cells treated with a non-toxic compound, flunisolide (left) and a toxic compound, pseudobaptigenin (right). B) BMDMs treated with IFN- $\gamma$  5 days following training produce negligible amounts of TNF- $\alpha$  in high-throughput screen. There was no significant difference between cells treated with only DMSO compared to those treated with any library compounds. C)  $\beta$ -glucan as whole glucan particles (WGP) induces trained immunity responses. BMDMs trained with WGP exhibit a 1.7-fold increase in TNF- $\alpha$  production relative to untrained control in a high-throughput screening context.

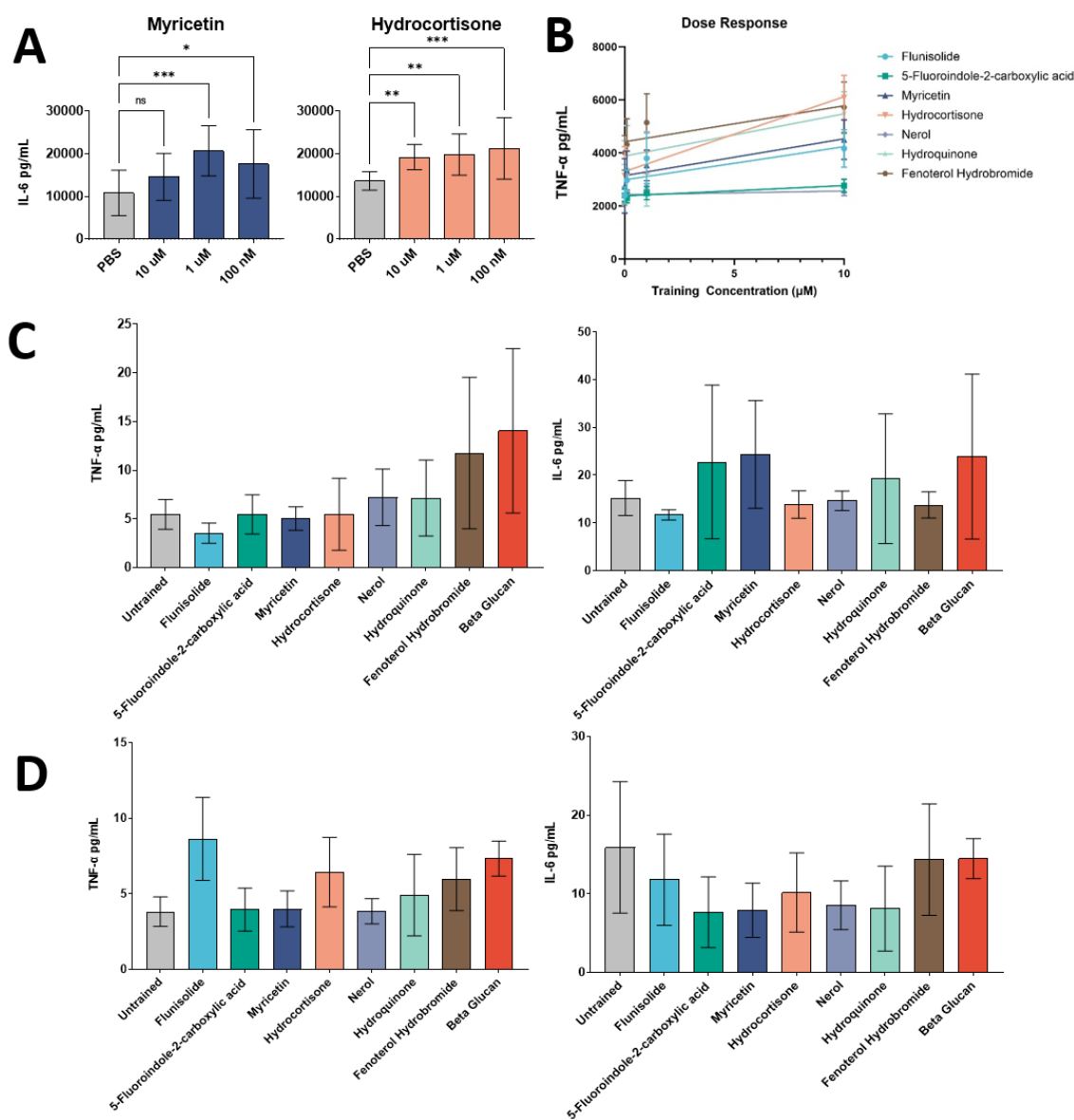


**Fig. S2.** A) Representative increases in IL-6 production. Small-molecule training results in increased production of IL-6 following challenge with 100 ng/mL Pam3. B) For each compound except nerol, there is a significant positive dose response from 100 nM to 10 μM ( $p < .0001$ ). C) Small molecules do not induce significant pro-inflammatory cytokine production. TNF- $\alpha$  and IL-6 were measured from BMDM cell culture supernatant 24 h following treatment with small molecules or  $\beta$ -glucan. D) BMDMs treated with IFN- $\gamma$  5 days following training produce negligible amounts of proinflammatory cytokines. There was no significant difference between cells treated with only DMSO compared to those treated hit compounds or  $\beta$ -glucan.

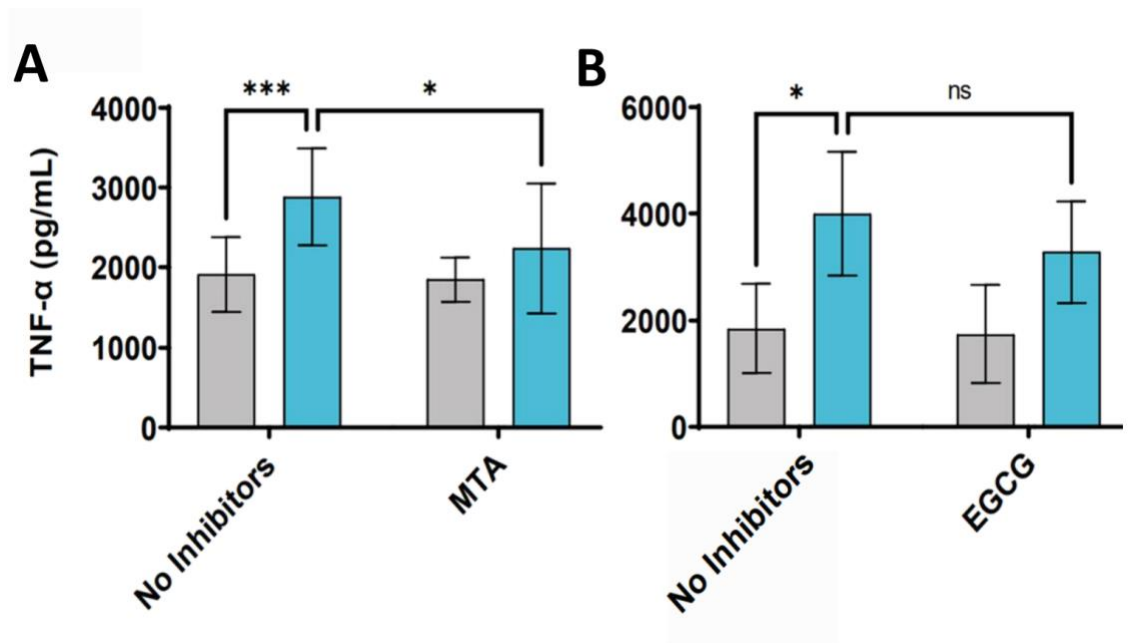


**Figure S3.** Epigenetic inhibition assay using MTA or EGCG and measuring TNF- $\alpha$  concentration following Pam3 challenge in cells trained with 10  $\mu$ M small molecules after 1h of pre-treatment with PBS or MTA ( $n = 15$ ). A) Flunisolide -induced training is inhibited by treatment with MTA. B) Flunisolide-induced training is not significantly inhibited by treatment with EGCG.

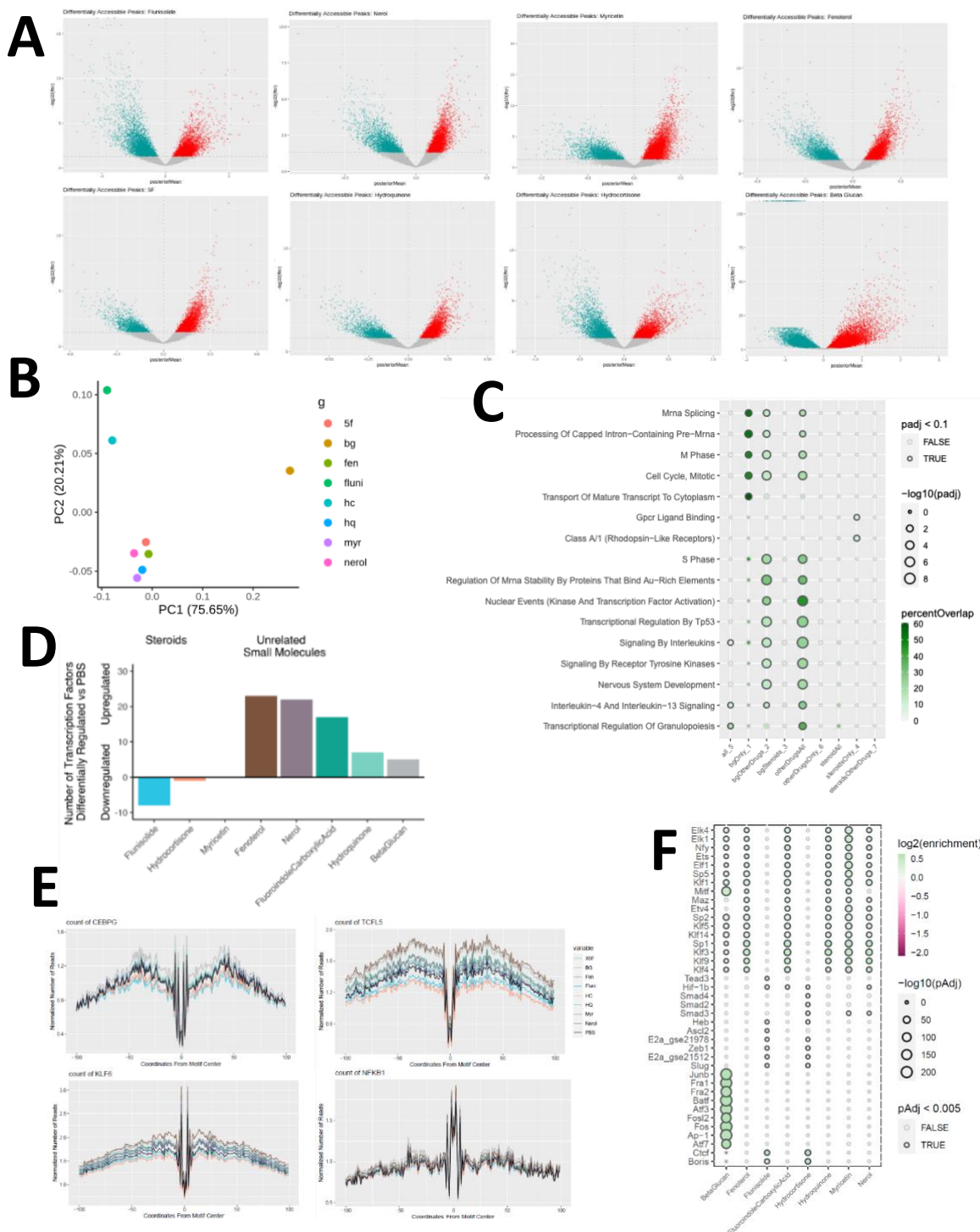


**Figure S4.** A) In vitro treatment of BMDMs with hit compounds results in differentially accessible chromatin. Significant differentially accessible peaks (LFSR <0.05) are shown in volcano plots as upregulated (red) or downregulated (blue) for each compound. B) Changes in chromatin accessibility are distinct between treatments. PCA from mashr betas showing  $\beta$ -glucan, glucocorticoids, and the remaining hit compounds clustering in separate areas of the multidimensional space. C) Analysis of overlapping genes identifies shared pathways. Signaling by IL-4 and IL-13 is more accessible in BMDMs treated with each compound, whereas glucocorticoids uniquely increase accessibility of GPCR ligand binding and rhodopsin-like receptors. D) Number of upregulated or downregulated TFs relative to PBS-treated control. Glucocorticoids result in downregulated TF binding, while other small molecules and  $\beta$ -glucan result in upregulated TF binding (Benjamini-Hochberg adjusted  $p < 0.1$ ). E) Example traces of

KLF6, CEBPG, and TCFL5 showing differential occupancy in footprinting analysis. F) Differential accessibility of TF binding sites by treatment condition in trained BMDMs.

**Dataset S1 (repository).** Raw fastq sequencing results of ATACseq on replicates of each of 7 treatments, raw and normalized counts files, as well as bed files for all peaks per replicate.

**Dataset S2 (separate file).** Adjusted p value and mean beta (modeled log fold change versus PBS treatment) for each peak per treatment from *mash* analysis of differential accessibility.

**Dataset S3 (separate file).** Adjusted p values for two-list over-representation analysis of significantly upregulated genes present in REACTOME database pathways versus a background of all genes proximal to peaks measured in this ATACseq experiment, per treatment condition.

**Dataset S4 (separate file).** Adjusted p values, JASPAR motifs, and fold changes among significant differentially regulated transcription factors from footprinting analysis for transcription factor occupancy in trained vs. untrained BMDMs, per treatment condition.